

Low-temperature solid-phase crystallization of amorphous silicon thin films deposited by rf magnetron sputtering with substrate bias

Seung-Ik Jun and Philip D. Rack^{a)}

Department of Materials Science and Engineering, The University of Tennessee, Knoxville, Tennessee 37996-2200

Timothy E. McKnight, Anatoli V. Melechko, and Michael L. Simpson

Molecular Scale Engineering and Nanoscale Technologies Research Group, Oak Ridge National Laboratory, Oak Ridge, Tennessee 37831

(Received 17 January 2006; accepted 1 June 2006; published online 10 July 2006)

The crystallization properties of amorphous silicon (*a*-Si) thin film deposited by rf magnetron sputter deposition with substrate bias have been thoroughly characterized. The crystallization kinetics for films deposited with substrate bias is enhanced relative to unbiased *a*-Si by films. The enhanced crystallization for substrate biased *a*-Si films are attributed to ion enhanced nucleation of crystallites during sputter deposition which subsequently grow during the postdeposition anneal. Conversely films sputter deposited without substrate bias have more intrinsic defects and residual oxygen which enhance nucleation and retard growth, respectively, and lead to a large number of small crystallites. © 2006 American Institute of Physics. [DOI: 10.1063/1.2219136]

Thin film transistors are widely used as a switching element for microelectronic applications and electronic display devices such as thin film transistor-liquid crystal displays (TFT-LCDs).¹ Many applications are divided between two silicon TFT technologies which depend on the ordering of the semiconducting Si active region: (1) hydrogenated amorphous silicon (*a*-Si:H) TFTs and (2) polycrystalline silicon (poly-Si) TFTs. To improve the field effect mobility, the *a*-Si film is usually crystallized by postannealing techniques such as solid-phase crystallization (SPC),² metal induced crystallization (MIC),³ metal induced lateral crystallization (MILC),⁴ field aided lateral crystallization (FALC),⁵ and excimer laser annealing (ELA).⁶

Kimura *et al.* proposed that the crystallization characteristics of *a*-Si vary with the stress state of the as-deposited *a*-Si films.⁷ Hashemi *et al.* demonstrated a crystallization method called stress-assisted nickel-induced crystallization.⁸

In our previous work, we showed that the properties of sputter deposited thin films such as metal,⁹ silicon oxide,¹⁰ and silicon¹¹ can be significantly changed with the addition of substrate bias during sputtering deposition. In this study, we demonstrate that ion irradiation induced by substrate biased during sputter deposition of *a*-Si films enhances the kinetics of crystal growth and the grain size of poly-Si film when crystallized by thermal annealing.

An AJA ATC2000 rf magnetron sputtering system equipped with four magnetron sources and a heated and/or dc biased substrate holder was used for the *a*-Si film deposition. The rf power and deposition temperature for all depositions were fixed at 200 W and 200 °C, respectively, and the substrate biases were 0 W (no substrate bias) and 30 W (215 V) during the deposition. A quartz tube furnace was used for thermal annealing and the conditions were atmosphere ambient and 600–900 °C every 100 °C for 20 h.

The XRD result of crystallized Si without substrate bias, as shown is Fig. 1(a), has a characteristic peak at $2\theta=28.5^\circ$ above 600 °C, and the intensity of XRD increases slightly with the annealing temperature. The intensity of the peak

is very small, and other characteristic peaks are not shown even at a high-temperature annealing of $\sim 900^\circ\text{C}$. We speculate that the crystallites are nanocrystalline with very small grain size. In contrast, the XRD spectra of crystallized Si deposited with substrate bias (30 W and 215 V), in Fig. 1(b), show strong characteristic peaks at $2\theta=28.5^\circ$, 47.5° , and 56.3° that correspond to (111), (220), and (311), respectively. The intensity of crystallized Si deposited with substrate bias is much higher and sharper than the films deposited without substrate bias which means high crystallinity in the poly-Si films.

Figure 2 shows UV reflectance spectra of annealed *a*-Si deposited with and without substrate bias. The change in the profile and the shift in the peaks in UV spectra indicate the modification of electronic density of states as a result of the long-range order. In the crystalline silicon, there are two main optical transition peaks: indirect transitions (E_1) at ~ 360 nm and direct transition (E_2) at ~ 273 nm.^{12,13} As shown in the figure, the characteristic peaks at both 273 and 360 nm are clearly shown in crystallized Si deposited with substrate bias and though the intensity is lower it resembles the single Si reference spectrum. The characteristic peaks, however, are not observed in the annealed Si deposited without substrate bias, and it indicates that the Si film is mostly amorphous or nanocrystalline at best.

Figures 3(a) and 3(b) show the spectra of Raman spectroscopy obtained by confocal micro-Raman spectroscopy (Renishaw 1000 spectrometer). The crystalline fraction of poly-Si, χ , was calculated roughly from the expression below,¹⁴

$$\chi = \frac{I_p}{I_p + \gamma I_a},$$

where I_p and I_a are integrated Raman scattering intensities of crystalline and amorphous silicon, respectively, and γ is the ratio of the integrated Raman cross section for poly-Si to *a*-Si. Tsu *et al.* suggested that the value of γ is 0.88 when the grain size or crystalline fraction is small.¹⁴ The crystallinities of the Si films with biased and unbiased at 600 °C for 20 h, as shown in Fig. 3, are 0.61 and 0.48, respectively. The net

^{a)}Electronic mail: prack@utk.edu

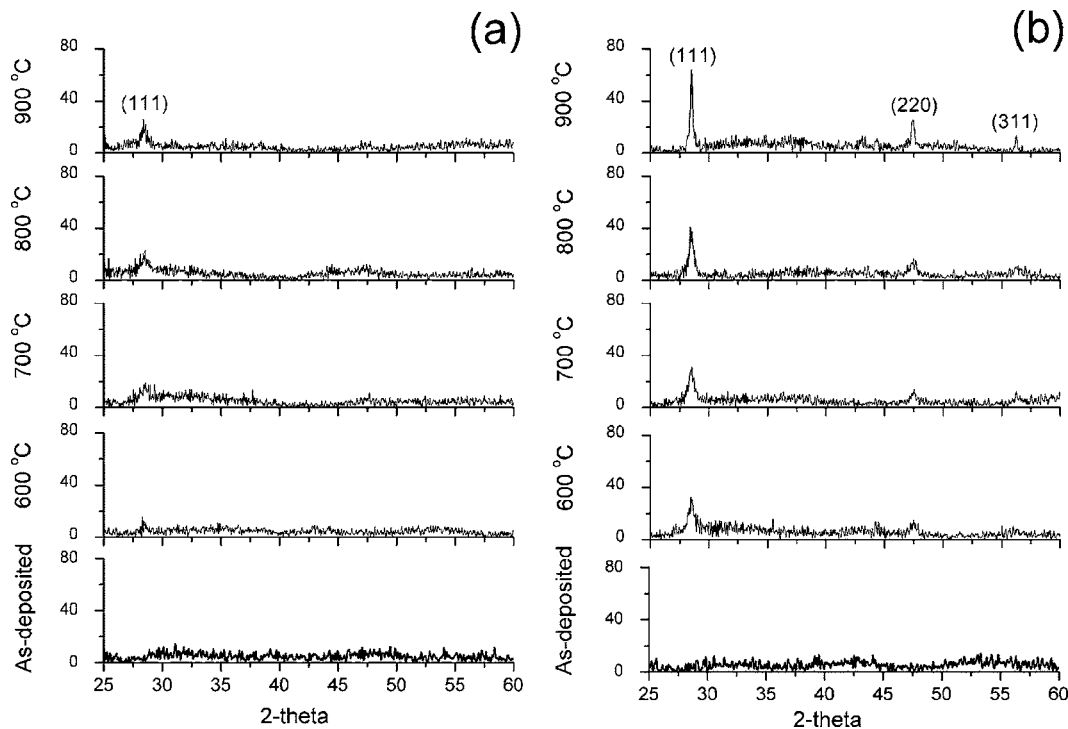


FIG. 1. (a) XRD spectra of annealed Si films deposited by unbiased sputter deposition and (b) XRD spectra of annealed Si films deposited by 30 W (215 V) biased sputter deposition.

crystallinity of crystallized Si deposited by substrate bias, however, is likely higher than this calculation result because the grain size of the poly-Si is larger and thus the γ value would be smaller than 0.88 that was used in the calculation (Fig. 4).

The Raman spectrum for the unbiased film annealed at 600 °C for 20 h has two characteristic peaks: a sharp poly-Si peak at 520 cm^{-1} and broad Raman shifted *a*-Si peak at 480 cm^{-1} . On the other hand, the crystallized Si from the 30 W biased *a*-Si film has only the sharp characteristic peak at 520 cm^{-1} for poly-Si. In the case of 900 °C (20 h), the *a*-Si peak is not observed in both crystallized films; however,

the biased poly-Si film has a narrower peak than the unbiased film indicating that the biased film is more crystalline under equivalent annealing condition.

To compare the microstructure of crystallized Si deposited with and without substrate bias, the surface morphology of the two films taken by SEM and AFM is shown in Fig. 4. The *a*-Si films were annealed and crystallized by SPC at 900 °C for 20 h in atmosphere ambient in a quartz tube furnace. The poly-Si film from substrate biased sputtering, as shown in the figure, has more condensed and larger grain size than those of unbiased poly-Si film.

The crystallization kinetics of amorphous Si is a very complex process and depends significantly on the stress state, impurities, preexisting crystalline nuclei, the underlying substrate (amorphous versus a crystalline silicon seed layer), and the defect structure in the amorphous silicon.¹⁵ In the crystallization of amorphous silicon without a preexisting crystalline interface or micro- or nanocrystalline nuclei, the phase transition from *a*-Si to poly-Si proceeds via random nucleation of crystalline clusters surrounded by the amorphous phase. In our previous work, we have shown that the properties of sputter deposited thin films can be significantly changed with the addition of substrate bias during sputter deposition.⁹⁻¹¹ The sputter deposition rate decreases, and the microstructure is densified (grain size also increases) with the addition of substrate bias.⁹ At low temperatures conventional sputter deposition without substrate bias generally leads to the formation of larger number of defects such as dislocations, vacancies, and stacking faults in the film relative to biased sputter deposition. For films deposited without substrate bias, these defects are the main centers for homogeneous nucleation and, as a result of the enhanced nucleation, the grain size of crystallized Si is small as observed in Fig. 4. For films sputter deposited with substrate bias, there are several factors that lead to the observed enhanced crys-

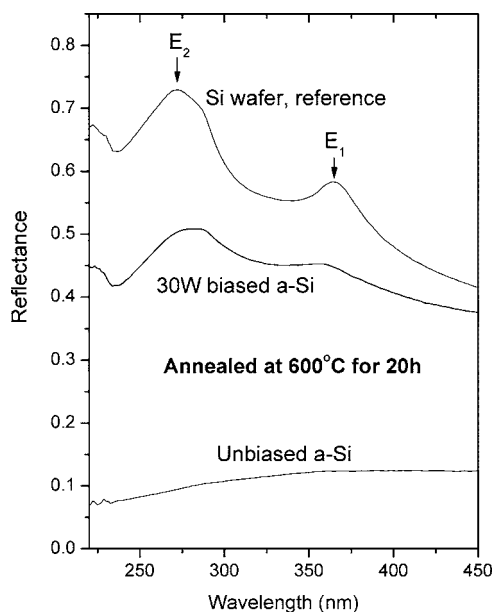


FIG. 2. UV reflectance spectra of annealed Si films deposited by unbiased and biased sputter deposition.

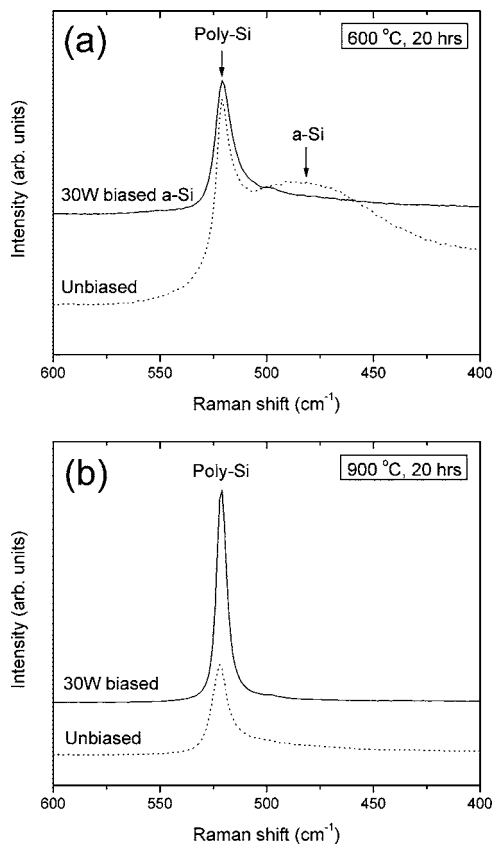


FIG. 3. (a) Raman spectra of annealed Si films deposited by unbiased and biased sputter deposition (annealed at 600 °C for 20 h) and (b) Raman spectra of annealed Si films deposited by unbiased and biased sputter deposition (annealed at 900 °C for 20 h).

tallization. First of all, during deposition at 200 °C, ion bombardment during growth can induce the nucleation of Si crystallites which is consistent with ion beam induced epitaxial crystallization results.¹⁶ These nuclei (either heterogeneous at the quartz interface or homogeneous in the film bulk) subsequently enhance the grain growth during the postdeposition anneal. Because there are fewer defects in the films sputtered with substrate bias, the homogeneous nucleation during the annealing is suppressed which results in a larger grain size as observed in Fig. 4. Finally, another possible contributing factor could be the residual oxygen concentration in the films. Ion bombardment during sputter deposition is known to reduce oxygen incorporation in as-deposited films. Oxygen (and other impurities such as C and F) is known to retard the silicon solid-phase crystallization process.^{17–19}

In conclusion, we showed that the crystallization kinetics is enhanced by biasing the substrate of sputter deposited *a*-Si thin films. In addition to the crystallinity, the grain size of poly-Si from substrate biased *a*-Si is much larger than that from unbiased *a*-Si. The enhanced grain size and crystallinity for substrate biased films are attributed to ion enhanced nucleation of crystallites during sputter deposition and growth of these nuclei during the postdeposition anneal. Conversely, films without substrate bias have more defects and residual oxygen which will enhance the nucleation and inhibit the growth, respectively, which lead to the observed smaller grain size.

This work was supported in part by the National Institute for Biomedical Imaging and Bioengineering under Assign-

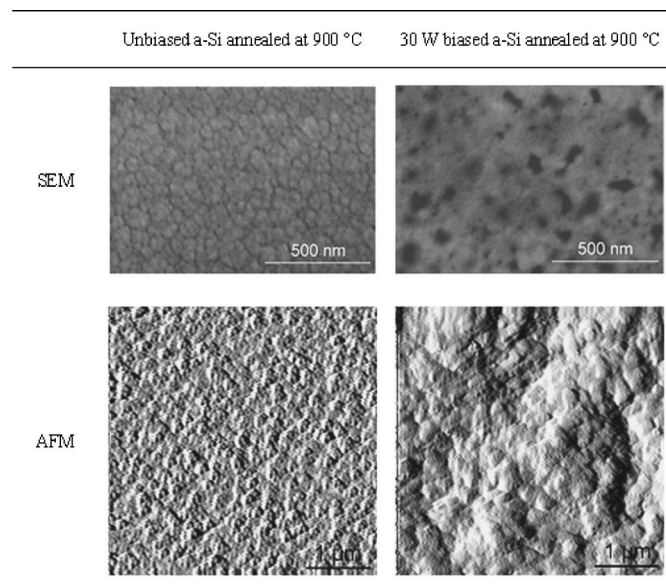


FIG. 4. Surface morphology of annealed Si films taken by SEM and AFM.

ment No. 1-R01EB000433-01 and through the Laboratory Directed Research and Development funding program of the Oak Ridge National Laboratory, which is managed for the U.S. Department of Energy by UT-Battelle, LLC. Two of the authors (A.V.M. and M.L.S.) acknowledge support from the Material Sciences and Engineering Division Program of the DOE Office of Science. A portion of this research was conducted at the Center for Nanophase Materials Sciences, which is sponsored at Oak Ridge National Laboratory by the Division of Scientific User Facilities, U.S. Department of Energy. The authors would like to thank to Dr. Ilia Ivanov, Darrell Thomas, Dale Hensley, and Dr. Yingfeng Guan for valuable contributions to this work.

¹Y. Kuo, J. Electrochem. Soc. **142**, 186 (1995).

²G. Farhi, M. Aoucher, and T. Mohammed-Brahim, Sol. Energy Mater. Sol. Cells **72**, 551 (2002).

³Y. Z. Wang and O. O. Awadelkarim, Appl. Phys. A: Mater. Sci. Process. **70**, 587 (2000).

⁴A. R. Joshi, T. Krishnamohan, and K. C. Saraswat, J. Appl. Phys. **93**, 175 (2003).

⁵S.-I. Jun, Y.-H. Yang, J.-B. Lee, and D.-K. Choi, Appl. Phys. Lett. **75**, 2235 (1999).

⁶M. Miyasaka and J. Stoemenos, J. Appl. Phys. **86**, 5556 (1999).

⁷Y. Kimura, M. Kishi, and T. Katoda, J. Appl. Phys. **86**, 2278 (1999).

⁸P. Hashemi, J. Derakhshandeh, S. Mohajerzadeh, M. Robertson, and A. Tonita, J. Vac. Sci. Technol. A **22**, 966 (2004).

⁹S.-I. Jun, P. D. Rack, T. E. McKnight, A. V. Melechko, and M. L. Simpson, J. Appl. Phys. **97**, 54906 (2005).

¹⁰S.-I. Jun, T. E. McKnight, A. V. Melechko, M. L. Simpson, and P. D. Rack, Electron. Lett. **41**, 822 (2005).

¹¹S.-I. Jun, P. D. Rack, T. E. McKnight, A. V. Melechko, and M. L. Simpson, Appl. Phys. Lett. **87**, 132108 (2005).

¹²M. Cardona and F. H. Pollak, Phys. Rev. **142**, 530 (1966).

¹³C.-H. Kuo, I.-C. Hsieh, D. K. Schroder, G. N. Maraoas, S. Chen, and T. W. Sigmon, Appl. Phys. Lett. **71**, 359 (1997).

¹⁴R. Tsu, J. Gonzalez-Hernandez, S. S. Chao, S. C. Lee, and K. Tanaka, Appl. Phys. Lett. **40**, 534 (1982).

¹⁵C. Spinella, S. Lombardo, and F. Priolo, J. Appl. Phys. **84**, 5383 (1998).

¹⁶J. S. Custer, A. Battaglia, M. Saggio, and F. Priolo, Phys. Rev. Lett. **69**, 780 (1992).

¹⁷G. L. Olson and J. A. Roth, Mater. Sci. Rep. **3**, 1 (1988).

¹⁸I. Suni, G. Goltz, M. G. Grimaldi, M.-A. Nicolet, and S. S. Lau, Appl. Phys. Lett. **40**, 269 (1982).

¹⁹M. Wittmer, J. Roth, P. Revesz, and J. W. Mayer, J. Appl. Phys. **49**, 5207 (1978).